Reduced work functions in gold electromigrated nanogaps

A. Mangin, A. Anthore, M. L. Della Rocca,* E. Boulat, and P. Lafarge
Matériaux et Phénomènes Quantiques, Université Paris Diderot-Paris 7, CNRS UMR 7162, 75205 Paris Cedex 13, France
(Received 30 July 2009; revised manuscript received 4 November 2009; published 29 December 2009)

We present current voltage measurements of clean electromigrated gold nanogaps at cryogenic temperatures. In all samples, we observe low voltage values (<1 V) for the crossover from direct tunneling to field emission regime. Two different tunneling models well explain the data with work functions values reduced with respect to the bulk ones. The influence of adsorbates on the metal work function in nanogaps is discussed.

DOI: 10.1103/PhysRevB.80.235432 PACS number(s): 73.40.Rw, 73.63.Rt

Electromigration in a metal wire subject to a high current density is the process in which atoms of the metal move due to the momentum transfer from the electrons, leading eventually to the breaking of the wire. Controlled electromigration has been successfully applied to nanowires for fabricating nanoscale gaps between metallic electrodes and it is a common method for realizing single molecule transistors.[1–3] A large number of phenomena have been observed in electromigrated single molecule devices such as Coulomb blockade and Kondo effect,[4,5] molecular vibrational modes spectroscopy,[6,7] light-induced effects,[8] magnetoresistance behavior,[9] and more recently, quantum magnetic phase transition.[10] These experiments raise the question of the appropriate description of electron transport through the nanogap in the tunneling regime without a molecule. Since criteria for probing the nature of a molecule are signatures in transport properties at specific energies, the knowledge of the behavior of bare nanogaps would clarify the interpretation of experiments on single molecule transistors. Although electrical characterizations have been performed on bare electromigrated nanogaps,[11,12] detailed measurements of their conduction properties have not been reported. In this work we present a careful analysis of the current voltage characteristics of fresh gold electromigrated nanogaps measured at low temperature over a large voltage range and compare them to theoretical calculations. We describe transport properties in the framework of electron tunneling through a trapezoidal barrier and we show that barrier heights much lower than the work function of gold are necessary to explain the data. Possible origins of this reduction are discussed considering similar results obtained in scanning tunneling microscopy (STM) and mechanically controllable break junctions (MCBJ).

Gold nanowires with a 50 nm$\times$20 nm constriction are made by electron beam lithography and double angled gold evaporation [see Fig. 1(a)]. The nanowire is located directly on the oxidized Si substrate or on a thin layer of alumina, covering an aluminum gate previously patterned. Controlled electromigration described in Ref. 13 is then performed at room temperature [Fig. 1(c)]. As shown in the inset of Fig. 1(c), during the last step of the electromigration process, the sample conductance evolves abruptly and displays plateaus at fractions of the conductance quantum $G_0=2e^2/h$ due to the formation of few channels contact when atoms are rearranging.[14,15] Eventually the process is stopped when the conductance reaches 0.1–0.2 G_0. This electromigration procedure has been tested either in air or in vacuum ($P<10^{-5}$ mbar) giving the same results.

A total of 107 samples has been measured at liquid helium temperature immediately after the electromigration process. Among them, 60 are discarded in the following analysis since they exhibit signatures of gold clusters trapped inside the gap. The current-voltage ($I-V$) characteristics of two representative examples of the remaining 47 samples with tunnel resistance 125 MΩ and 140 GΩ are shown, respectively, in Figs. 2(a) and 2(b). They display the characteristic features of electronic transport through a potential barrier in metallic tunnel junctions. Assuming an initial potential barrier with a trapezoidal shape [see insets in Fig. 2(c)], at voltage lower than the barrier height direct tunneling occurs giving rise to a linear increase in the current with the voltage. When the applied bias is higher than the barrier height, electrons tunnel through a triangular barrier instead of a trapezoidal one. Since the tunneling probability depends exponentially on the barrier width, the dominant term in the $I-V$ dependence becomes exponential.[16] This is the so-called field-emission or Fowler-Nordheim regime.[17] As shown in Fig. 2(c), the transition from direct tunneling to field emission is clearly evidenced in a plot of $\ln(I/V^2)$ vs $1/V$ by the

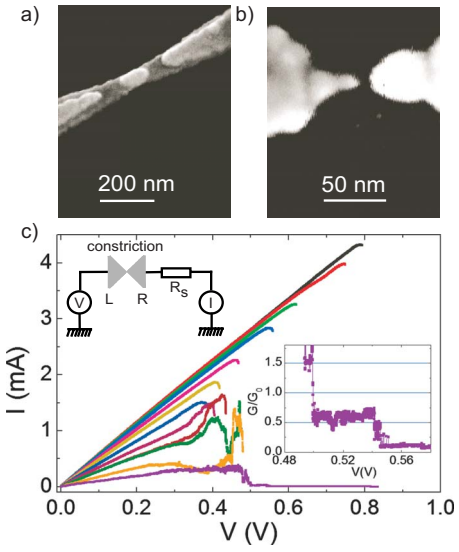

FIG. 1. (Color online) (a) Scanning electron microscope image of the constriction in sample Nano1 before electromigration. (b) Typical SEM image of a nanogap after electromigration and measurements at low temperature. (c) Current-voltage characteristics during the electromigration process. Right inset: conductance plateaus observed during the last ramp. Left inset: schematic representation of the electromigration and measurements setup. The $R_S=150$ Ω series resistance is due to the wiring.

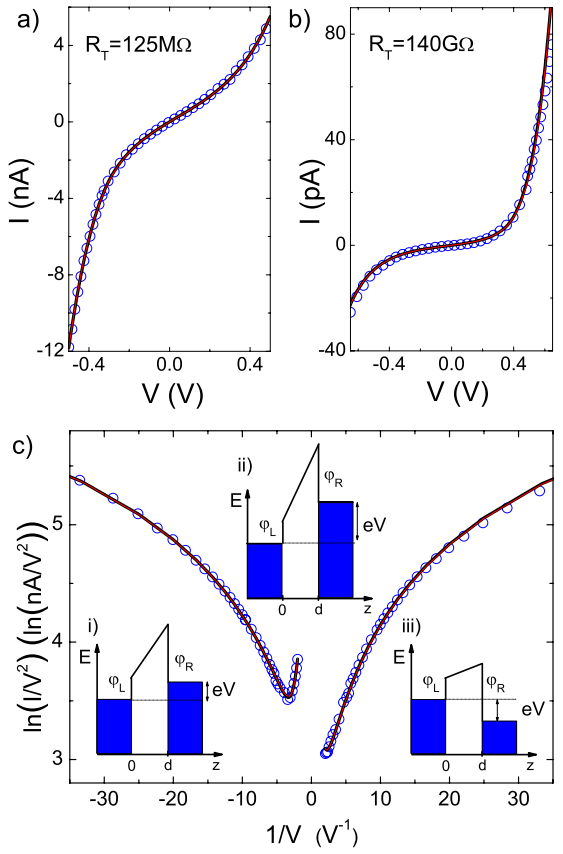

FIG. 2. (Color online) (a) and (b): current-voltage characteristic of sample Nano1 and Nano5 (open blue dots). (c): Data of sample Nano1 in the Fowler-Nordheim representation. The shape of the tunnel barrier used to model transport is represented in three different region (i) $-\varphi_L < V < 0$, (ii) $V < -\varphi_L$, (iii) $0 < V < \varphi_R$. Solid lines: fits to the 1D model (black) and to the planar junction model (red) with $A = 10$ nm^2. Curves are not distinguishable. The used fit parameters for the 1D (planar) model are $\varphi_L = 0.29$ eV(0.23 eV), $\varphi_R = 0.95$ eV(1 eV), and $d = 1.18$ nm(1.31 nm) for sample Nano1 and $\varphi_L = 1.24$ eV(1.25 eV), $\varphi_R = 0.35$ eV(0.31 eV), and $d = 1.79$ nm(1.88 nm) for sample Nano5.

presence of a minimum. In a first approximation, the voltage value corresponding to the crossover provides an estimation of the barrier heights of the electrodes.[18,19] For the data shown in Fig. 2(c), the crossover is not present for the positive voltage range, meaning that the barrier height of the right electrode is higher than the maximum voltage explored (0.5 V). The curves are generally asymmetric indicating different barrier heights on the left and right electrodes and the voltage at minimum varies from sample to sample.

In order to compare $I-V$ characteristics with theoretical calculations, we consider transport in the nanogap as a scattering problem. Within the Landauer-Büttiker formalism,[20] the current in the nanogap is expressed as

$$I(V) = \frac{2e}{h}\int_0^{+\infty} dE[f_L(E) - f_R(E)] \times \sum_{i=1}^{N} T_i(E,V). \qquad (1)$$

Here, f_L and f_R are the Fermi distributions of electrons in, respectively, the left and right electrode, N is the number of conduction channels and $T_i(E,V)$ is the transmission probability through the barrier for an incoming electron in channel i with total energy E when a bias voltage V is applied. To perform the calculations, two geometries were used: one-dimensional (1D) and planar. The observation of conductance steps characteristic of atomic contacts at the end of electromigration suggests that before breaking the constriction is ballistic with a size comparable to the Fermi wavelength λ_F.[14,15] Assuming the nanogap maintains this geometry, a 1D model is suitable to describe transport in our systems. In the limit of a single transmission channel ($N = 1$), Eq. (1) reads[20,21]

$$I(V) = \frac{2e}{h}\int_0^{+\infty} [f(E) - f(E - eV)]T(E,V)dE. \qquad (2)$$

On the other hand, when the sample is cooled down, the resistance usually increases. This might be due to local surface instabilities and atomic diffusion in the electrodes leading to an increase in the cross section and size of the nanogap. For a planar junction, with a cross section A larger than λ_F^2, Eq. (1) can be rewritten using a free electron model as

$$I(V) = \frac{4\pi mAe}{h^3}\int_0^{+\infty} dE[f(E) - f(E - eV)]\int_0^{E} T(E_z,V)dE_z, \qquad (3)$$

where m is the electron mass, $E = E_z + E_\perp$ is the total energy of electrons, which is split in a perpendicular component $E_\perp$ and a component E_z, longitudinal to the tunneling direction. The transmission probability $T(E_z,V) = T(E - E_\perp, V)$ does only depend on E_z by virtue of the invariance of the problem with respect to translation in the plane of the junction. This form of the tunneling current is the widely used Simmons model.[16,22]

The current in both models mainly depends on the electron transmission probability across the barrier $T(E,V)$. In the Wentzel Kramers Brillouin (WKB) approximation, this probability is given by

$$T(E,V) = \exp\left\{-\int_{s_1}^{s_2} \frac{4\pi}{h}\sqrt{2m[\varphi(z,V) - E]}dz\right\}, \qquad (4)$$

where $\varphi(z,V)$ is the potential profile along the tunnel barrier, and s_1 and s_2 are the turning points coordinates, solutions of the equation $\varphi(z,V) - E = 0$.

In our calculations, we use a tilted trapezoidal barrier model. The three parameters are the work functions of the left electrode φ_L, the right electrode φ_R, and the barrier width d. The potential profile at applied voltage V is then $\varphi(z,V) = \varphi_L + (\varphi_R - \varphi_L - eV)z/d$. This is the minimal model describing the main quantitative features observed in the current voltage dependence, namely, the asymmetry of the curves and the crossover from direct tunneling to field-emission regime. Nevertheless, this description of the nanogap is oversimplified since we do not take into account the image potential which would reduce the height and thickness of the potential barrier and round its shape.

The fit to the experimental data through Eqs. (2) and (3) are shown in Fig. 2 as solid black (red) lines for the

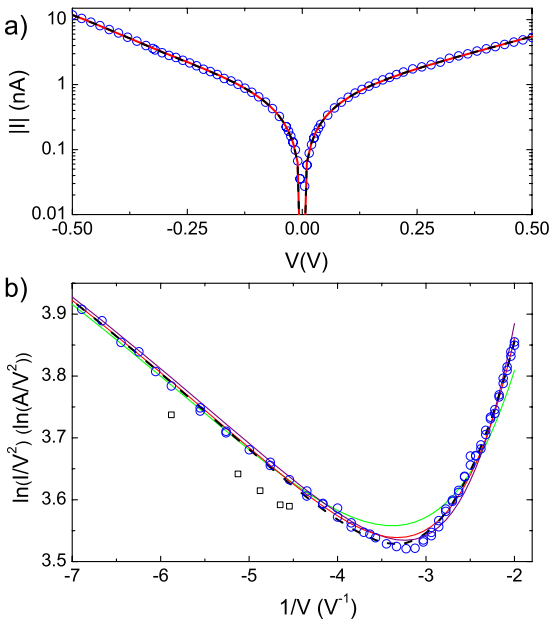

FIG. 3. (Color online) (a) Current-voltage characteristic of sample Nano1 (open blue dots) on a logarithmic scale compared to the fits based on the 1D model (black dashed line) and the planar junction model (red line). (b) Expanded view of the data (open dots and squares) of sample Nano1 near the minimum of the Fowler-Nordheim representation. Black dashed line: fit to the 1D model using the following parameters $\varphi_L=0.29$ eV, $\varphi_R=0.95$ eV, and $d=1.18$ nm. Solid colored lines: fit to the planar junction model when varying the area A of the nanogap cross section (from top to bottom at the minimum, green $A=1$ nm^2, red $A=10$ nm^2, and purple $A=100$ nm^2). The best fit is obtained for $A=10$ nm^2, $\varphi_L=0.23$ eV, $\varphi_R=1.00$ eV, and $d=1.31$ nm.

1D (planar) model. We used a steepest descent method to minimize the average squared difference value χ^2 to the experimental data. In order to compare the two models on different samples, data are equally weighted in the whole voltage range by normalizing contributions to the χ^2 by the experimental uncertainty. Note that the fitting procedure has been tested also on data in the Fowler-Nordheim representation giving the same results. In Figs. 2 and 3(a), the 1D and the planar fits are not distinguishable, both are in very good agreement with experimental data over three orders of magnitude. For sample Nano1 [Fig. 2(a)], the extracted values for the 1D (planar junction) model are $\varphi_L=0.29$ eV(0.23 eV), $\varphi_R=0.95$ eV(1 eV) and $d=1.18$ nm(1.31 nm), while for sample Nano5 [Fig. 2(b)], we find for the 1D (planar junction) model $\varphi_L=1.24$ eV(1.25 eV), $\varphi_R=0.35$ eV(0.31 eV) and $d=1.79$ nm(1.88 nm). When fitting with the planar model, the cross section parameter is set to $A=10$ nm^2 for both samples. The parameter A is a prefactor to the exponential current dependence of Eq. (3), therefore, it has only a weak influence on the shape of the $I-V$ curve. Some criteria on plausible area can be set: for a planar model to hold, the nanogap cross section must be larger than λ_F^2. For gold, λ_F is smaller than one nanometer, as a consequence, we assume, as a lower bond $A_{\min}=0.1$ nm^2. At the same time, one can put an upper bound on A based on inspection of scanning electron microscope (SEM) images [see Fig. 1(b)] taken after warming up allowing an estimation the maximum nanogap area $A_{\max}$. The cross section A should be smaller than $A_{\max}$. Typical values of $A_{\max}$ range from 100 nm^2 to 1000 nm^2.

For a closer comparison of the two models, we focus in Fig. 3(b) on the data of sample Nano1 in the region of the minimum in the Fowler-Nordheim plot. This region is the most sensitive part of the $I-V$ curve to the shape of the tunnel barrier. First, note the existence of some points, represented as open black squares, which belong to a different metastable configuration of the nanogap and are not considered in the fitting procedure. Many samples show such multiple unstable configurations. In Fig. 3(b), the black dashed line is the best fit obtained with the 1D model. For the planar model, we used three different values of the cross section $A(1,10,100$ nm$^2)$ between $A_{\min}$ and $A_{\max}$. For each value of A, the best fit is plotted as a solid colored line. Even if the parameter A has only a weak influence on the shape of the $I-V$ curve, the Fowler-Nordheim plot displays variations in the curves related to different A values. The fits for the planar junction with $A=10$ nm^2 (red curve) and the 1D model superpose perfectly at low and high voltage, they slightly differ in the minimum region where the 1D model provides lower values. The highest discrepancies appear clearly in the minimum region as well as at high voltages for $A=1$ nm^2 (green line). For $A=100$ nm^2 (purple line), discrepancies are less visible but still exist close to the minimum and at very high voltages.

We have carried out a similar detailed analysis between the two models on six different samples with resistances ranging from 125 MΩ to 185 GΩ. Results are summarized in Table I. Based on the above discussion on sample Nano1, we use $A=10$ nm^2 when fitting with the planar model. This choice is supported by the fact that for each sample, the two models give similar χ^2 values. The extracted barrier heights vary by less than 0.1 eV except for sample Nano3 and the barrier width varies by less than 0.2 nm between the two models. Even if our analysis cannot infer the exact nanogap size, these findings indicate that we determine the effective barrier width and heights with a maximum relative uncertainty of, respectively, 10% and 20%. Note that an increase in the tunnel resistance R_T is not correlated with an increase in the barrier width. Furthermore, the fact that the two models give consistent results in describing the data is understandable by considering that the dominant term both in Eqs. (2) and (3) is the transmission probability $T(E,V)$ of electron crossing the tunnel barrier. This term does not depend on the nanogap cross section A and it has the same exponential expression in both models as shown in Eq. (4).

The fits performed on samples Nano1 to Nano6 result in typical effective barrier heights smaller than 2 eV. The average value obtained after fitting the $I-V$ curves of 47 nanogaps is 0.7 eV. These values are significantly smaller than the work function of bulk gold metal ~5 eV. Image forces, not taken into account in our calculation, are known to reduce the barrier height and width. The barrier reduction obtained with the usual expression of the image potential does not exceed 2 eV for a 1 nm thick tunnel junction,[23] this is not sufficient to explain the large reduction observed. Besides,

TABLE I. Fit parameters for the samples used in this work. The tunnel resistance is measured at 4.2 K. For the 1D model, the three fit parameters are the barrier heights of the electrodes (φ_L and φ_R) in eV and the barrier width d in nm. For the planar model the nanogap cross section is set to $A=10$ nm^2.

Sample	R_T (GΩ)	Model	φ_L (eV)	φ_R (eV)	d (nm)
Nano1	0.125	1D	0.29	0.95	1.18
		planar	0.23	1.00	1.31
Nano2	0.3	1D	1.06	0.79	1.01
		planar	1.07	0.78	1.15
	2	1D	3.71	0.51	0.84
Nano3		planar	3.97	0.40	0.95
Nano4	3	1D	0.29	0.41	2.04
		planar	0.27	0.39	2.14
Nano5	140	1D	1.24	0.35	1.79
		planar	1.25	0.31	1.88
Nano6	185	1D	1.56	0.36	1.67
		planar	1.62	0.29	1.77

we found that the planar model fit is poorer when image forces are included. This suggests that, although image forces certainly have an influence on the tunnel barrier, proper calculations of the potential profile in nanogaps should use an *ab initio* approach taking into account the geometry of the electrodes.

A more appropriate explanation for reduced work functions could be the presence of adsorbates on the electrodes of the nanogap. A 10^{-5} mbar pressure during the electromigration procedure is not low enough to ensure the absence of carbon, hydrogen, nitrogen, and oxygen based compounds in the sample environment.[24] A long standing issue in literature is the influence of adsorbates on transport properties of nanometric size contacts measured in MCBJ, STM experiments and nanowire based STM-like devices. It is commonly accepted that the signature of adsorbates is a nonlinear $I-V$ behavior at low voltage, which could be interpreted as a lowering of the tunnel barrier height due to reduced work functions. For example, in STM-like experiments in air, atomic size contacts with $G \ll G_0$ have non linear $I-V$ curves in a similar voltage range as in our measurements.[25] Besides, tunneling like $I-V$ characteristics have also been observed in MCBJ in UHV when molecules are previously linked to the electrodes.[26,27] In this particular case, the nonlinear $I-V$ characteristics can be explained by a structure where the molecule does not directly connect the two electrodes but rather acts as an extension of the electrodes with electrons still tunneling through the vacuum. This picture supports the idea that a thin layer of organic molecules always contaminate the sample surface inhibiting the formation of a true metal-vacuum-metal junction.[28] Yet, no work functions were inferred from the data mentioned above. A quantitative estimation of gold work functions has been reported mainly in STM experiments. A reduction comparable to our findings has been measured in pure water,[29] electrolyte solutions,[30] as well as in air.[31] In these experiments, reported work functions are between 0.1 and 2 eV, lower than the bulk value of 5 eV found in ultraclean transport experiments.[32,33] All these observations tend to prove that the reduced work functions arise from the contamination of the metallic surface. From a theoretical point of view, molecular dynamics simulations are not able to completely account for the work function reduction observed in literature as well as in our work. Different theoretical works have studied the influence of water[34,35] and the effect of monolayers of different molecules.[36] The lower effective barrier height calculated in the jellium model for a thin layer of water (0.96 nm) between two metallic planes is 2 eV.[34] Recently, it has been demonstrated that the adsorption of impurities on metal surfaces (Cu) can induce a significant reduction in the work function independently of their electroaffinity as a result of polarization and Pauli exclusion effect.[37]

Another effect known to produce a reduction in work functions is the presence of defects on the surfaces leading to the definition of a local non homogeneous work function.[38] In ultraclean conditions, a 0.1 eV work function has been found at the position of missing rows in the gold surface reconstruction.[39] In our experiments, the crystal structure of the electrodes is not regular and a similar effect could take place. A full theoretical interpretation of our results is still lacking.

Our work shows that the experimental issue of work functions lowering in various realization of nano tunnel junction is also relevant for nanogaps formed by electromigration. We

draw attention to the importance of characterizing transport properties of bare electromigrated nanogaps since most of single molecule experiments are performed with electromigrated samples in similar working conditions as ours. A correct interpretation of transport properties in the presence of a molecule needs to wash out all spurious effect related to the structure itself.

In conclusion, we have shown that gold nanogaps fabricated by electromigration exhibit current-voltage characteristics consistent with tunneling through a trapezoidal potential barrier with low work functions. Our results show that a 1D as well as a planar junction model can describe the whole current voltage characteristic for samples with very different tunnel resistances. The consistency of the two models suggests that the nanogap structure is at the crossover between planar and one dimensional geometry with a 10 nm^2 cross section. The observed reduction in the effective potential barrier and the asymmetry of the current-voltage characteristics demonstrate the importance of the crystal structure of the electrodes and impurity adsorption in transport experiments based on metallic nanogaps. Our results suggest that further theoretical work is needed to explain the work function reduction in atomic size tunnel junction.

This work is supported by Grant No. ANR-05-JCJC-0149-01 and by the C'Nano Ile de France SPINMOL contract. We gratefully acknowledge helpful discussions with D. Esteve, the Quantronic groups, W. Wernsdorfer, F. Balestro, M. Aprili, and M.F. Goffman, and we thank C. Ciuti for critical reading of the manuscript.

*maria-luisa.della-rocca@univ-paris-diderot.fr

[1] H. Park, A. K. L. Lim, A. P. Alivisatos, J. Park, and P. L. McEuen, Appl. Phys. Lett. **75**, 301 (1999).
[2] D. R. Strachan, D. E. Smith, D. E. Johnston, T.-H. Park, M. J. Therien, D. A. Bonnel, and A. T. Johnson, Appl. Phys. Lett. **86**, 043109 (2005).
[3] K. O'Neill, E. A. Osorio, and H. S. J. van der Zant, Appl. Phys. Lett. **90**, 133109 (2007).
[4] J. Park, A. N. Pasupathy, J. I. Goldsmith, C. Chang, Y. Yaish, J. R. Petta, M. Rinkoski, J. P. Sethna, H. D. Abruña, P. L. McEuen, and D. C. Ralph, Nature (London) **417**, 722 (2002).
[5] E. A. Osorio, T. Bjornholm, J.-M. Lehn, M. Ruben, and H. S. J. van der Zant, J. Phys.: Condens. Matter **20**, 374121 (2008).
[6] H. Park, J. Park, A. K. L. Lim, E. H. Anderson, A. P. Alivisatos, and P. L. McEuen, Nature (London) **407**, 57 (2000).
[7] E. A. Osorio, K. O'Neill, N. Stuhr-Hansen, O. F. Nielsen, T. Bjornholm, and H. S. J. van der Zant, Adv. Mater. **19**, 281 (2007).
[8] D. R. Ward, N. J. Halas, J. W. Ciszek, J. M. Tour, Y. Wu, P. Nordlander, and D. Natelson, Nano Lett. **8**, 919 (2008).
[9] A. N. Pasupathy, R. C. Bialczak, J. Martinek, J. E. Grose, L. A. K. Donev, P. L. McEuen, and D. C. Ralph, Science **306**, 86 (2004).
[10] N. Roch, S. Florens, V. Bouchiat, W. Wernsdorfer, and F. Balestro, Nature (London) **453**, 633 (2008).
[11] M. F. Lambert, M. F. Goffman, J. P. Bourgoin, and P. Hesto, Nanotechnology **14**, 772 (2003).
[12] F. Prins, T. Hayashi, B. J. A. de Vos van Steenwijk, B. Gao, E. A. Osorio, K. Muraki, and H. S. J. van der Zant, Appl. Phys. Lett. **94**, 123108 (2009).
[13] A. Mangin, A. Anthore, M. L. Della Rocca, E. Boulat, and P. Lafarge, J. Appl. Phys. **105**, 014313 (2009).
[14] J. M. Krans, J. M. van Ruitenbeek, V. V. Fisun, I. K. Yanson, and L. J. de Jongh, Nature (London) **375**, 767 (1995).
[15] U. Landman, W. D. Luedtke, B. E. Salisbury, and R. L. Whetten, Phys. Rev. Lett. **77**, 1362 (1996).
[16] J. G. Simmons, J. Appl. Phys. **34**, 1793 (1963).
[17] R. H. Fowler and L. Nordheim, Proc. R. Soc. London, Ser. A **119**, 173 (1928).
[18] J. M. Beebe, B. S. Kim, J. W. Gadzuk, C. D. Frisbie, and J. G. Kushmerick, Phys. Rev. Lett. **97**, 026801 (2006).
[19] P.-W. Chiu and S. Roth, Appl. Phys. Lett. **92**, 042107 (2008).
[20] Y. M. Blanter and M. Büttiker, Phys. Rep. **336**, 1 (2000).
[21] J. J. W. M. Rosink, M. A. Blauw, L. J. Geerligs, E. van der Drift, and S. Radelaar, Phys. Rev. B **62**, 10459 (2000).
[22] R. Stratton, J. Phys. Chem. Solids **23**, 1177 (1962).
[23] M. C. Payne and J. C. Inkson, Surf. Sci. **159**, 485 (1985).
[24] P. S. Anufriev, D. Boltenkov, and C. Ryabinkov, Tech. Phys. **51**, 100 (2006).
[25] J. Abellán, R. Chicón, and A. Arenas, Surf. Sci. **418**, 493 (1998).
[26] C. A. Martin, D. Ding, H. S. J. van der Zant, and J. M. van Ruitenbeek, New J. Phys. **10**, 065008 (2008).
[27] E. Lörtscher, H. B. Weber, and H. Riel, Phys. Rev. Lett. **98**, 176807 (2007).
[28] K. Hansen, S. K. Nielsen, M. Brandbyge, E. Lægsgaard, I. Stensgaard, and F. Besenbacher, Appl. Phys. Lett. **77**, 708 (2000).
[29] M. Hugelmann and W. Schindler, Surf. Sci. **541**, L643 (2003).
[30] D. H. Woo, E. M. Choi, Y. H. Yoon, K. J. Kim, I. C. Jeon, and H. Kang, Surf. Sci. **601**, 1554 (2007).
[31] S. C. Meepagala and F. Real, Phys. Rev. B **49**, 10761 (1994).
[32] O. Yu. Kolesnychenko, O. I. Shklyarevskii, and H. van Kempen, Phys. Rev. Lett. **83**, 2242 (1999).
[33] L. Olesen, M. Brandbyge, M. R. Sørensen, K. W. Jacobsen, E. Lægsgaard, I. Stensgaard, and F. Besenbacher, Phys. Rev. Lett. **76**, 1485 (1996).
[34] W. Schmickler, Surf. Sci. **335**, 416 (1995).
[35] I. Benjamin, D. Evans, and A. Nitzan, J. Chem. Phys. **106**, 6647 (1997).
[36] V. De Renzi, Surf. Sci. **603**, 1518 (2009).
[37] P. S. Bagus, D. Käfer, G. Witte, and C. Wöll, Phys. Rev. Lett. **100**, 126101 (2008).
[38] N. D. Lang, Phys. Rev. B **37**, 10395 (1988).
[39] R. Schuster, J. V. Barth, J. Wintterlin, R. J. Behm, and G. Ertl, Ultramicroscopy **42-44**, 533 (1992).